

Glutathione transferase P1-1 as an arsenic drug-sequestering enzyme

Lorien J. Parker,^{1,2} Alessio Bocedi,³ David B. Ascher,¹ Jade B. Aitken,⁴ Hugh H. Harris,⁵ Mario Lo Bello,⁶ Giorgio Ricci,³ Craig J. Morton,¹ and Michael W. Parker^{1,2*}

¹ACRF Rational Drug Discovery Centre, St. Vincent's Institute of Medical Research, Fitzroy, Victoria 3065, Australia

²Department of Biochemistry and Molecular Biology, Bio21 Molecular Science and Biotechnology Institute, The University of Melbourne, Parkville, Victoria 3010, Australia

³Department of Chemical Sciences and Technologies, University of Rome "Tor Vergata", Rome 00133, Italy

⁴School of Chemistry, The University of Sydney, Sydney, New South Wales 2006, Australia

⁵Department of Chemistry, The University of Adelaide, Adelaide, South Australia 5005, Australia

⁶Department of Biology, University of Rome "Tor Vergata", Rome 00133, Italy

Received 6 October 2016; Accepted 14 November 2016

DOI: 10.1002/pro.3084

Published online 18 November 2016 proteinscience.org

Abstract: Arsenic-based compounds are paradoxically both poisons and drugs. Glutathione transferase (GSTP1-1) is a major factor in resistance to such drugs. Here we describe using crystallography, X-ray absorption spectroscopy, mutagenesis, mass spectrometry, and kinetic studies how GSTP1-1 recognizes the drug phenylarsine oxide (PAO). In conditions of cellular stress where glutathione (GSH) levels are low, PAO crosslinks C47 to C101 of the opposing monomer, a distance of 19.9 Å, and causes a dramatic widening of the dimer interface by approximately 10 Å. The GSH conjugate of PAO, which forms rapidly in cancerous cells, is a potent inhibitor ($K_i = 90$ nM) and binds as a di-GSH complex in the active site forming part of a continuous network of interactions from one active site to the other. In summary, GSTP1-1 can detoxify arsenic-based drugs by sequestration at the active site and at the dimer interface, in situations where there is a plentiful supply of GSH, and at the reactive cysteines in conditions of low GSH.

Keywords: arsenic; glutathione transferases; inhibitors; resistance; X-ray crystallography

Introduction

Glutathione transferases (GSTs; EC 2.5.1.18) are a key part of the antioxidant response system.^{1,2} Their principal mode of detoxification is through catalyzing the conjugation of target compounds to

glutathione (GSH) as a first step in the removal of toxins from cells. In addition, GSTs can also protect cells by binding toxic compounds, through noncatalytic sequestration mechanisms. Due to the high expression levels of GSTs in many cells, this

Additional Supporting Information may be found in the online version of this article.

C.J.M. and M.W.P. are senior co-authors.

Grant sponsors: Commonwealth of Australia under the Major National Research Facilities Program (Australian Synchrotron Research Program), U.S. DOE, Basic Energy Sciences, Office of Energy Research (Use of the Advanced Photon Source), Australian Research Council (financial support), High Energy Accelerator Research Organization (KEK) in Tsukuba, Japan (operations support), Research Council (ARC), the Australian Cancer Research Foundation (to M.W.P.), the Victorian Government Operational Infrastructure Support Scheme to St. Vincent's Institute and from MIUR and Genesys SpA (to M.L.B.), National Health and Medical Research Council of Australia (NHMRC), Dora Lush Scholarship, and International Centre for Diffraction Data Crystallography Scholarship (to L.J.P.), Australian Postgraduate Award and St Vincent's Foundation Scholarship (to D.B.A.).

*Correspondence to: Michael Parker, St. Vincent's Institute of Medical Research, Fitzroy, Victoria 3065, Australia. E-mail: mparker@svi.edu.au

particular ligandin function may contribute to toxin resistance more significantly than previously considered. GSTs have been strongly implicated in various cancers; for example, in several tumor cell lines there is substantial overexpression of these enzymes following exposure to antitumor drugs.¹⁻³ Acquired resistance, which eventually arises in patients after an initial period of successful anticancer treatment, has been related in some cases to the presence of GST enzymes.⁴

Arsenic is a human carcinogen causing cancers of the skin, lung, bladder, liver, and kidney after long-term exposure. Toxic exposure to arsenic is a serious health problem in some parts of the world where it occurs either naturally or as a pollutant.⁵ Although arsenic is well-known for its properties as a human carcinogen, arsenicals have also been used as therapeutic agents for thousands of years.^{6,7} Up until the early 1900s arsenic was used as the primary antileukemic agent until it was replaced by radiation therapy and more modern chemotherapy. Arsenicals made a comeback in the early 1970s when they were used successfully for the treatment of acute promyelocytic leukemia (APL). Arsenic trioxide (As₂O₃, Trisenox) was approved for treatment of APL in 2000 for patients who fail to respond to other chemotherapy methods or have relapsed disease.⁸ This recent success has prompted researchers to consider arsenic's application in the treatment of other malignant disorders including chronic lymphocytic leukemia, multiple myeloma,^{9,10} and solid tumors such as neuroblastoma,¹¹ gastric,¹² and cervical tumors.¹³

Cells can develop tolerance to arsenicals¹⁴⁻¹⁶ and a correlation between GSTP1-1 overexpression and development of resistance to arsenicals has been described by a number of workers. For example, the level of arsenic resistance in an arsenic-resistant mammalian cell line is correlated with expression levels of GSTP1-1, and GST inhibitors markedly decrease cell resistance to the metalloid.¹⁷ It has been shown that the enzyme is directly involved in excretion of arsenic from cells.¹⁸ Furthermore, acquired self-tolerance to arsenic in chronically exposed cells is associated with increased expression of GSTP1-1 and multidrug resistance transporters.¹⁹ Inhibition of the enzyme markedly increases arsenic accumulation and arsenic toxicity, indicating the enzyme's upregulation is critical for acquired tolerance in cells chronically exposed to arsenic.¹⁹ GSTP1-1 has been shown to block As₂O₃-induced apoptosis in leukemia, prostate cancer and lymphoma cells.²⁰⁻²² *In vivo* studies have shown that GSH serves as a reducing agent for the conversion of arsenate to arsenite, and that GST activity is involved in the metabolism of arsenic by catalyzing the formation of arsenic-GSH conjugates.^{23,24} The tri-GSH conjugate As(GS)₃, is recognized and pumped out of the cell by multidrug resistant pump 1. Leslie *et al.*²⁵ showed that GSTP1-1 was required for

transport of As(III) (plus GSH) providing substantive evidence that the formation of As(GS)₃ might be catalyzed by GSTP1-1.

The organic arsenical, phenylarsine oxide (PAO), is a membrane-permeable phosphotyrosine phosphatase inhibitor that is active in hematopoietic cells.²⁶ Several groups have reported the cytotoxic effects of PAO in hematological malignancies.²⁶⁻²⁸ The cytotoxic effect of PAO is nine times higher than As₂O₃, and this toxicity does not weaken toward As₂O₃-resistant cell lines.²⁹ These results suggested that PAO may be a promising new agent for the treatment of APL, particularly for APL patients who are resistant and refractory to As₂O₃ treatment. However, PAO's high toxicity and nonselectivity for cancer cells over normal cells are drawbacks to be overcome in any drug development program. Recently, an analog of PAO (4-(*N*-(*S*-glutathionylacetyl)amino)phenylarsonous acid) has been tested in phase I clinical trials for solid tumors that are refractory to standard therapy.³⁰

It is now well-established that in human cancers, arsenic detoxification is performed by the GST/GSH detoxification system. However, the interaction of GSTP1-1 with arsenic-based drugs is surprisingly poorly characterized. Here we describe crystallography, X-ray absorption spectroscopy, mass spectrometry, mutagenesis, and kinetics of GSTP1-1's interactions with PAO. A crystal structure of PAO bound to GSTP1-1 in the absence of GSH shows the region corresponding to helix α 2, which contains the C47 residue, is disordered, consistent with PAO interacting with this reactive cysteine and causing the displacement of this region from its usual helical conformation. Binding is associated with a dramatic opening of the V-shaped dimer cleft. Furthermore, the extended X-ray absorption fine structure (EXAFS) and crystallographic studies suggest that PAO can crosslink C47 of one monomer to C101 of the neighboring monomer. Kinetic studies reveal that the GSH adduct of PAO binds in the active site of the enzyme and is one of the most potent inhibitors of GSTP1-1 so far described in the literature. The crystal structure of the PAO complex, in the presence of GSH, reveals that PAO binds as a di-GSH-phenyl arsenic complex at the active site of the enzyme. In addition, PAO interacts at the dimer interface with C101 of either subunit resulting in the formation of a continuous network of interactions that spans from one active site to the other. This is the first report of a GSTP1-1 inhibitor that can simultaneously block known ligand binding sites in both the active sites and dimer interface. Overall, the structures reveal that GSTP1-1, in the presence of GSH, can detoxify PAO in two ways: by binding di-GSH-phenyl arsenic at the G-site and by sequestering PAO alone at the dimer interface. In the absence of GSH, detoxification occurs through binding to the two reactive cysteine residues, C47 and

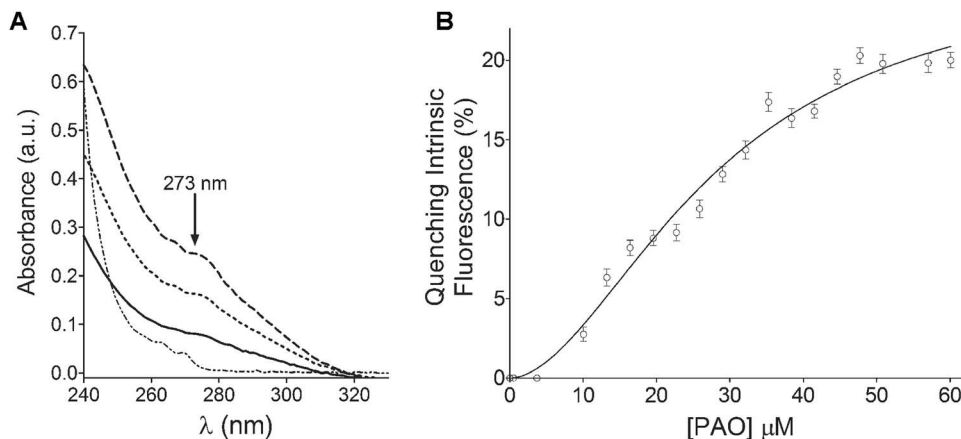


Figure 1. Kinetic studies of PAO binding to GSTP1-1. (A) UV absorption spectra of PA(GS)₂ complex. 1 mM GSH was reacted with variable amounts of PAO 33 μM (—), 66 μM (---), 100 μM (····) in 0.1M potassium phosphate buffer, pH 6.5. The spectrum of PAO alone (100 μM) is also reported (-·-·-·). (B) Binding of PAO to GSTP1-1 was followed on the basis of the quenching of intrinsic fluorescence at 344 nm ($\lambda_{\text{exc.}} = 295$ nm). GSTP1-1 (1 μM) was incubated with variable amounts of PA(GS)₂ (from 3 to 60 μM) in 0.1M potassium phosphate buffer, pH 6.5 (25°C). [PAO]_{0.5} = 28 μM; $n_{\text{H}} = 1.85$. Experiment was performed in triplicate (i.e., three different spectrophotometric determinations performed on three distinct samples). Error bars represent SEM.

C101. The structures provide a basis for the development of GST inhibitors that block all these sequestration modalities.

Results

The di-GSH adduct of PAO is a potent inhibitor of GSTP1-1

In healthy and cancerous cells, GSH is present at millimolar concentrations. Thus we first explored how human GSTP1-1 recognizes PAO in the presence of its substrate GSH. In the presence of 1 mM GSH and substoichiometric amounts of PAO (0.1 mM) at pH 6.5, the PA(GS)₂ complex is rapidly formed in a few seconds ($t_{1/2} < 1$ s). The complex is characterized by a typical UV spectrum with a maximum at 210 nm and a shoulder at 273 nm ($\epsilon_{\text{M}} = 2500 \text{ M}^{-1} \text{ cm}^{-1}$) [Fig. 1(A)]. The instability constant of the complex (K_{inst}), calculated as described in Materials and Methods section, is $1.6 \times 10^{-9} \text{ M}^2$. When incubated with GSTP1-1, this compound behaves as a strong competitive inhibitor of GSTP1-1 toward GSH ($K_{\text{i}} = 90 \text{ nM}$) (Table I).

To verify the possible involvement of the two highly reactive cysteines (C47 and C101)³¹ in the

binding of the PA(GS)₂ complex, we measured the K_{i} values of the corresponding serine mutants of these two residues. The study suggests no direct interaction occurs between the mutated residues and the complex (Table I). In fact, the decreased affinity of the complex in these mutants is quantitatively similar to the loss of affinity for GSH in both mutants.

Mass spectrometry reveals two adducts in the GSTP1-1 PAO GSH complex

In the presence of GSH two reaction species with GSTP1-1 were observed by mass spectrometry: a minor species with mass of 458.58 Da and a major species of 765.33 Da (Supporting Information Fig. S1). The former corresponds to a monogluthionylated species of PAO whereas the latter corresponds to the digluthionylated species of PAO.

Crystal structure of the GSTP1-1 PAO GSH complex reveals multiple binding sites

We determined the crystal structure of the enzyme in complex with PAO and GSH to a resolution of 1.5 Å. The structure reveals that PAO interacts with GSTP1-1 at two different sites [Fig. 2(A,B)]. In the

Table I. Kinetic Data of PAO and PA(GS)₂ Binding to GSTP1-1 Wild-Type and Mutants

	K_{m} (M)	K_{i} (M) ^a	[PAO] _{0.5} (M) ^b	n_{H} ^b
Wt	$1.2 \pm 0.2 \times 10^{-4}$	$9 \pm 2 \times 10^{-8}$	$28 \pm 11 \times 10^{-6}$	1.8 ± 0.2
C47S	$1.3 \pm 0.3 \times 10^{-3}$	$3.0 \pm 0.3 \times 10^{-6}$	$8 \pm 3 \times 10^{-6}$	1.9 ± 0.4
C101S	$2.7 \pm 0.4 \times 10^{-4}$	$3.5 \pm 0.4 \times 10^{-7}$	$15 \pm 6 \times 10^{-6}$	1.9 ± 0.3
C47S/C101S	$2.1 \pm 0.4 \times 10^{-3}$	—	$>10^{-4}$	—

Each experiment was performed in triplicate (i.e., three different spectrophotometric determinations on three distinct samples) and errors are SEM.

^a K_{i} is the inhibition constant for the competitive inhibition of GSTP1-1 (wt and mutants) by PA(GS)₂ complex.

^b [PAO]_{0.5}, that is, the concentration of the inhibitor that causes 50% of the fluorescence quenching at saturation. n_{H} are calculated from quenching fluorescence experiments of GSTP1-1 (wt and mutants) and PAO.

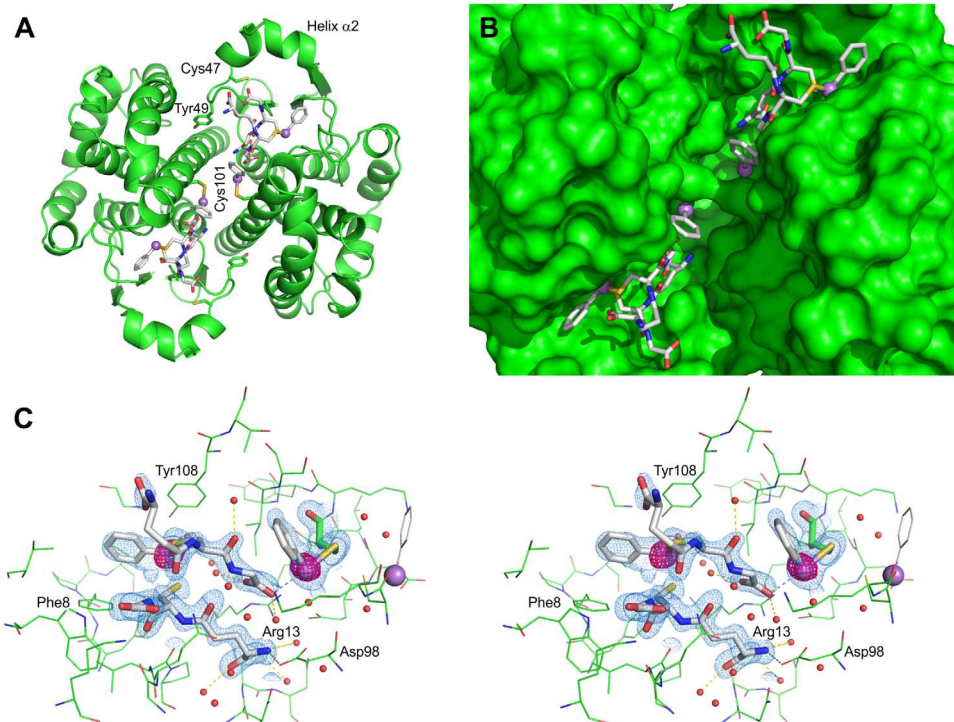


Figure 2. Crystal structure of the GSTP1-1-PAO-GSH complex. (A) Ribbon representation of GSTP1-1 showing the network of interactions across the dimer interface. The arsenic atoms are shown as purple spheres, GSH and the phenyl ligands and the reactive cysteines as sticks with atomic coloring. The locations of helix $\alpha 2$, the reactive cysteines, and the key residue Tyr 49 are also indicated. (B) Close-up view of the active site cleft, with the protein shown as a solvent-accessible surface and the GSH, arsenic, and phenyl ligands shown as in panel A. (C) Stereoview of the final $2F_o-F_c$ electron density map (contour level 1σ in blue) and anomalous difference Fourier maps (contour at 8σ in pink) of the diGSH-phenyl-arsenic complex bound in the active site of one chain in the GSTP1-1 dimer. Surrounding residues are shown as sticks and waters shown as red spheres. Putative hydrogen bonds between water molecules and the ligand are shown as yellow dashed lines, with direct bonding (intermolecular) interactions between the bound ligands and between the ligand and protein shown as grey dashed lines. Some key residues discussed in the text are labeled.

active site, PAO is observed as the di-GSH phenyl arsenic complex [Fig. 2(C)]. One of the GSH ligands, GSH1, binds in the G-site in the same way, with the same interactions, as seen in other GST-GSH complexes.^{32,33} The second GSH ligand, GSH2, binds in the active site in a head-to-tail direction with respect to the first GSH ligand. The GSH in the GSH2 site has a higher average temperature factor for its terminal glutamyl moiety (39 \AA^2) compared with the G-site GSH (21 \AA^2) which reflects the increased flexibility of this moiety and the relatively few contacts it makes with the protein as indicated by incomplete electron density [Fig. 2(C)]. The glycyl carboxylate moiety forms a salt bridge with the side chain of Arg13, and there are numerous van der Waals interactions with Ile104 and Tyr108. The phenyl group of the arsenic complex stacks between the aromatic rings of Phe8 and Tyr108 (distance between centroids of 4.5 \AA and 6 \AA , respectively) as well as forming van der Waals interactions with the main chain of Gly205 and the side chain of Val10 [Fig. 2(C)]. The arsenic atom is covalently bound through the sulfur atoms of the two GSH molecules, as well as the phenyl ring, and is within vicinity of

the hydroxyl of Tyr108 (3.2 \AA). GSH2 makes a water-mediated interaction with Asp98 from the other subunit. GSH1 makes water-mediated interactions with residues such as Pro53, Gln64, Asn66, and Glu97 in addition to the usual protein interactions seen in other GSH bound GST structures, (Supporting Information Fig. S2).

Two arsenic binding sites were also identified at the dimer interface, covalently bound to C101 of each subunit [Fig. 2(A,B)]. Reaction of PAO with a single thiol group would lead to a phenylhydroxy-arsene complex. There was some additional electron density attached to the arsenic peaks that was modeled as the phenyl moieties. The location of the hydroxyl was not well-defined so was not modeled in this structure. The extensive water network that is normally observed at the dimer interface in other GSTP1-1 structures is disrupted by binding of PAO. At occupancy of 0.6, the average temperature factor of the arsenic ions refined to 26 \AA^2 , similar to that of the C101 thiols (average of 28 \AA^2). The arsenic ions form a 2.6 \AA arsenic-sulfur bond with the thiol of C101 and are also within 3.0 \AA of the carboxylate group of the glycyl moiety of GSH2 (Fig. 2).

Binding of PAO to GSTP1-1 in the absence of GSH

In stressed cells, the levels of GSH can be very low so we examined how GSTP1-1 interacts with PAO at low GSH concentrations. Binding of PAO to GSTP1-1 was followed on the basis of the quenching of intrinsic fluorescence of the protein [Fig. 1(B)]. Interestingly, the isothermic binding is strongly cooperative with an Hill coefficient of 1.85 and a $[PAO]_{0.5} = 28 \mu M$ (Table I). We also evaluated the possible involvement of C47 or C101 on the binding of PAO. After replacing each of these residues separately with serine, the protein was still found to bind to PAO in a strongly cooperative process ($n_H = 1.87$) (Table I) with $[PAO]_{0.5}$ values close to that found for the wild-type protein, being $8 \mu M$ and $15 \mu M$ for the C47S and C101S mutants, respectively. However, as expected, the double mutant C47S/C101S does not bind to the compound up to $0.1M$ concentration.

Mass spectrometry reveals major and minor metalloid binding sites in the PAO only complex

In the absence of GSH several reaction products were observed, with one major species showing an increase in the deconvoluted mass of approximately 167 Da. This mass would be consistent with one phenylhydroxy-arsene-Cys complex per monomer. A minor species of 334 Da per monomer was observed and corresponds to two phenylhydroxy-arsene-Cys complexes per monomer. The kinetic (see above) and crystallographic studies (see below) are consistent with the major site of PAO reaction being at C47 and the minor site at C101. C47 has been shown previously to be the most reactive cysteine in apo GSTP1-1.³¹

Crystal structure of the GSTP1-1 PAO complex in the absence of GSH reveals metalloid binding at the dimer interface and displacement of helix $\alpha 2$

In the absence of GSH, electron density for the arsenic adduct is evident at the dimer interface, albeit at a low occupancy, bound to the thiol of C101 of each subunit [Fig. 3(A)]. The arsenic atoms refined to occupancies of 0.3 with an average temperature factor of 36 \AA^2 , close to those of the C101 thiols (average of 38 \AA^2). Interestingly, these sites are on the opposite side of the C101 thiols to that seen for the same peaks in the structure with GSH described above [Fig. 3(A,B)]. No electron density was evident for the phenyl ring or the hydroxy ligand, so they were excluded from refinement. The usual water network observed at the dimer interface in other GSTP1-1 structures is severely disrupted by binding of PAO, as was observed in the GSH-bound structure.

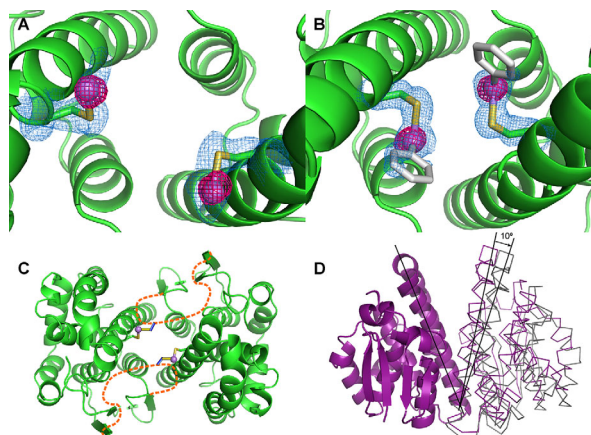


Figure 3. Crystal structure of the GSTP1-1-PAO complex. (A, B) Views of the final $2F_o - F_c$ electron density map (contour level 1σ in blue) and anomalous difference Fourier maps (contour at 8σ in pink) of PAO bound to Cys101 at the dimer interface. In panel A, the PAO complex structure is shown, and in panel B, the PAO-GSH complex is shown by way of comparison. (C) Ribbon representation of GSTP1-1 suggesting how PAO is able to crosslink monomers via the reactive cysteines. The arsenic atoms are shown as purple spheres with Cys101 as sticks with atomic coloring. The disordered helix- $\alpha 2$ is represented by the dashed orange line for both chains of the GSTP1-1 dimer, with the putative position of the other reactive cysteine Cys47 represented diagrammatically as a bond to the arsenic. (D) Superposition of subunit A of the GSTP1-1 GSH complex (PDB id: 5GSS) onto subunit A of the GSH-free PAO complex (ribbon depiction). The movements of subunit B of the GSH-free PAO complex (grey) with respect to the GSH-bound structure (purple) are depicted by alpha-carbon traces.

Strikingly, there is no electron density for the region corresponding to helix $\alpha 2$, (residues 35–50) suggesting it has become highly mobile and possibly disordered [Fig. 2(A,C)]. This region includes C47 and the kinetic studies showed that PAO reacts with this residue in the absence of GSH. In contrast, the same region in the GSH-bound structure described above is well-ordered, consistent with published kinetic studies that C47 becomes inaccessible in the presence of GSH.³¹ Thus we assume the absence of density in this region is a consequence of the G-site being empty and PAO binding to C47.

The C-terminal end of helix $\alpha 2$ includes Tyr49, a residue that has been described as a “key” that fits into a hydrophobic pocket (the “lock”) of residues contributed from the neighboring subunit [Fig. 2(A)].³² Mutational studies of Tyr49 show that it is a critical residue for stability of the GSTP1-1 dimer.³⁴ We visualize for the first time the consequences of removing the key from the lock: the cleft at the dimer interface has widened markedly with an increase in the separation at the tip of the helical towers of approximately 8 \AA . Superposition of the individual monomers onto the corresponding monomers in the GSH-bound structure described above

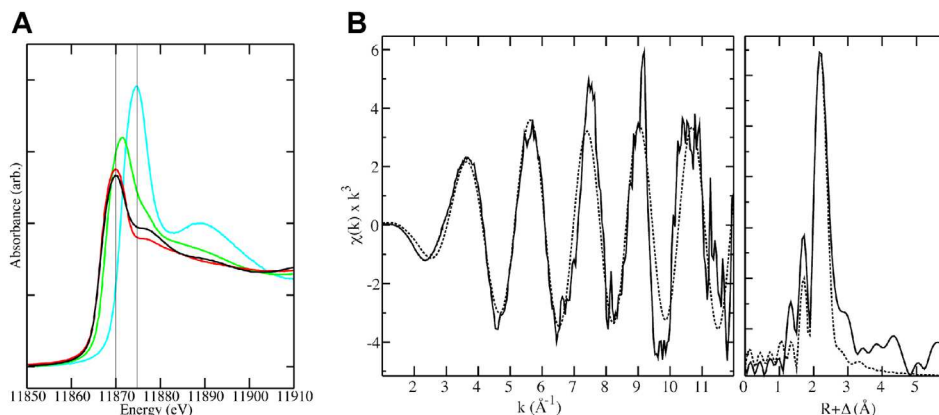


Figure 4. X-ray absorption spectroscopy of PAO binding to GSTP1-1. (A) As K-edge X-ray absorption near edge spectra for GST incubated with PAO in the absence of GSH (black trace), As(GS)_{3(aq)} (red), aqueous arsenite (green), and aqueous arsenate (blue). Vertical lines are drawn at 11,870 and 11,875 eV. (B) As K-edge EXAFS spectrum (left) and corresponding phase-corrected Fourier transform (right) of GST incubated with PAO in the absence of GSH. The calculated fit from model 1 in Supporting Information Table S1 is shown as the dotted trace in both k and R space.

indicates no significant changes in the monomeric structures (r.m.s.d. of ~ 0.3 Å). Superposition of one monomer of the PAO complex onto the published wild-type GSTP1-1 GSH complex structure (PDB id: 5GSS³³) reveals a rotation of approximately 10° of the second monomer with respect to the first, pivoting at the base of the helical tower [Fig. 3(D)]. Superposition of the GSH-bound and GSH-absent dimers reveals that while the residues at the base of the dimer superimpose closely, the upper half of the dimer has separated. The distance between the C101 carbon alpha atoms has increased from 7.8 Å in the GSH-bound structure to 11.2 Å in the GSH-free structure. We confirmed this observation by collecting a further three data sets, each from one crystal, of the GSH-free PAO complex and the widening of the dimer interface to the same degree was consistent throughout.

Crystal structure of the GSTP1-1 PAO complex from crystals grown in the absence of GSH and subsequently soaked in GSH

To determine if binding of GSH to the active site was sufficient to re-stabilize helix $\alpha 2$, which forms one wall of the G-site, we took a PAO soaked crystal, in the absence of GSH, after 2 days, and reintroduced GSH. This crystal was from the same drop as the crystal used for the PAO structure described above. To our surprise, back-soaking this crystal in GSH for 5 days restored the structure of the disordered helix, including the “lock-and-key” and re-stabilized the interaction between the monomers, resulting in a distance between the tips of the helical towers identical to that observed in published GSTP1-1 structures. C47 and C101 are no longer modified, presumably because the excess GSH competed with PAO at that site. Furthermore, many of the critical waters that are usually observed in the

dimer interface of other GSTP1-1 structures are again observed. This back-soaked structure has the di-GSH-phenyl arsenic species bound at each active site, each with an occupancy of 0.6 and average temperature factor of 25 Å².

Crystal structure of apo GSTP1-1

We next wanted to explore whether the absence of helix $\alpha 2$ and the widened interface were due to the absence of ligand in the G-site as such ligands are thought to stabilize the helix which forms one wall of the site. Although apo GSTP1-1 structures have previously been reported they were generated from crystals that were soaked in ligands that were not visible in the electron density maps. As it is possible that the ligands were still bound but disordered, we decided to solve an apo GSTP1-1 structure from crystals that were not soaked in any ligand. The structure shows good electron density for all regions of the protein, including helix $\alpha 2$ and the lock-and-key, and there is an extensive network of waters visible at the dimer interface and in the active sites. Although helix 2 can be observed, an analysis of temperature factors shows this region in both monomers is one of the most mobile regions in the structure in accord with published solution studies.^{35–37} The V-shaped dimer cleft resembles that seen in published GSTP1-1 structures. Thus the disappearance of helix $\alpha 2$ and the widened cleft seen in the PAO complex is not due to absence of ligand in the active site.

EXAFS studies reveal that PAO binding to GSTP1-1 in the absence of GSH results in the formation of two AS-S bonds

We undertook X-ray absorption spectroscopy (XAS) studies to determine the ligand environment of the arsenic binding sites in the enzyme. This study

could only be done in the absence of GSH since PAO reacts with GSH rapidly in solution. Our crystallographic, mass spectrometry, and kinetic studies, performed in parallel with the XAS studies, revealed that PAO could react with two sites (C47 and C101) on the enzyme. X-ray absorption near edge spectroscopic data [Fig. 4(A)] showed that the oxidation state of arsenic remains as As(III) when PAO is bound to the enzyme. The white line peak energy was found to be identical to that of aqueous As(GS)₃, but a comparatively lower peak intensity indicated a lower symmetry environment, consistent with a 2S,1C coordination shell.³⁸

Curve fitting analysis of extended X-ray absorption fine structure data (EXAFS) showed that arsenic was bound to two sulfur donor ligands at a bond distance of 2.24 Å in the GST-PAO complex (Supporting Information Table S1), with a model containing three As-S sulfur interactions producing a significantly greater fit error. Attempts to include an As-C fit component were complicated by strong EXAFS cancellation over the full data range with the longer distance As-S component, producing a characteristic minimum in the EXAFS Fourier transform at approximately 2 Å [Fig. 4(B)]. Nonetheless, a fit which included a fixed Debye-Waller factor for the As-C component produced an As-C bond distance of 1.93 Å which is consistent with the median distance (1.96 Å) for such a bond in the eighty examples of similar coordination environments (2S,1C-phenyl) found in the Cambridge crystallographic database.

The EXAFS data are consistent with PAO forming a crosslink between C47 and C101. Inspection of the structure suggests the crosslink is most likely between monomers and the location of the arsenic anomalous signal on the opposite side of C101 to that observed in PAO GSH complex also supports this interpretation [Fig. 3(A-C)].

Discussion

PAO is considered a promising agent for treating certain types of leukemia and solid tumors that are resistant to other anticancer drugs, with an analog currently in human clinical trials.³⁰ However, in cancer cells PAO is readily attacked by GSH and protein thiols such as those in GSTP1-1, a detoxifying enzyme that is overexpressed in many types of cancer cells at millimolar concentrations.^{1,2} Studies in yeast suggest that arsenic is mainly protein-bound in acute exposure situations whereas it is mainly GSH-bound after long-term exposure.³⁹ Thus GSTP1-1 may be a major cause of arsenic drug inactivation in human cancer cells. We show here that the GSH adduct of PAO is a potent inhibitor of GSTP1-1 with a K_i of 90 nM. We further show that the parent molecule, PAO, can react with C47 and C101 of the enzyme (Table I).

The crystal structure of GSTP1-1 complexed to PAO, in the presence of GSH, reveals four arsenic ligands bind to the enzyme, connected to each other via an extensive network of interactions [Fig. 2(A)]. Bond lengths between the arsenic atom and the GSH thiol atoms are approximately 2.4 Å, which is in accordance with the expected bond lengths for this interaction.⁴⁰ This structure is very similar to the published wild-type GSH complex structure (PDB id: 5GSS³³) with a r.m.s deviation in carbon α positions of 0.3 Å for 414 residues. Despite the accommodation of an additional GSH ligand, as well as the phenyl-arsenic moiety in the active site, no significant movements are observed for any of the active site residues.

In the absence of GSH, the crystal structure shows that PAO binds to the C101 ligands at the dimer interface with an arsenic-sulfur bond distance of 2.4 Å [Fig. 3(A)]. The enzyme appears less reactive with PAO in the absence of GSH, suggesting that the GSH-mediated interactions with the arsenic-bound C101, observed in the PAO-GSH complex, might facilitate and stabilize binding of arsenic at this site. Although C47 is not observed in the crystal structure our kinetic and mass spectrometry studies are consistent with PAO binding at this residue also. Mass spectrometry revealed a major reaction species in the absence of GSH that corresponds to one PAO per GST monomer and a second reaction species in the sample with two PAO per GST monomer. The crystallography data are consistent with C47 being the major site of PAO binding. EXAFS showed that arsenic was bound to two sulfur donor atoms at 2.2 Å and one carbon at 1.9 Å when PAO was incubated with GST in the absence of GSH (Fig. 4), indicating that the reaction resulted in the loss of the oxido ligand from PAO, but the retention of the phenyl group. Taken together the data support an intermonomer crosslink between C47 and C101 [Fig. 3(C)].

The most remarkable feature of the GSH-free PAO complex structure is the increase in width of the water-filled cleft at the dimer interface. Normally the distance between the α carbon atoms of residue 113, located at the top of the helical towers, is 22.3 Å but in the GSH-free PAO complex structure this distance is 28.2 Å [Fig. 3(D)].³³ The change in the dimer interface appears specific for PAO as the ligand was introduced by soaking pre-formed GST crystals using the same protocol that has been used previously for numerous other GST ligands, none of which resulted in a change to the dimer interface.^{33,41-45} Furthermore, the effect appears to be associated with PAO binding of C47 as binding at C101 in the presence of GSH did not cause any change to the dimer interface. This movement at the dimer interface is probably the cause of the strong cooperativity observed during PAO binding either to

wild-type or to the single Cys mutants. This homotropic cooperative interaction, mimics the one produced by 6-(7-Nitro-2,1,3-benzoxadiazol-4-ylthio)hexanol when it binds to GSTP1-1 in the absence of GSH⁴⁶ and is likely made possible by the lock-and-key motif present at the dimer interface.³⁴

A surprising feature of the GSH-free PAO complex is the absence of electron density for helix $\alpha 2$ (residues 35–50). Previously published “apo” human GSTP1-1 structures were derived from wild-type crystals soaked in ligands expected to bind in the active site giving rise to the doubt that the G-site was truly empty. Thus we decided to determine a new apo structure that revealed an intact helix $\alpha 2$. It thus seems likely that the disorder of helix $\alpha 2$ is associated with chemical modification of C47, which is known to be accessible only in the apoenzyme.³¹ Disruption of helix $\alpha 2$ by C47 modification with the more bulky PAO leads to withdrawal of the key residue, Tyr49, from its hydrophobic lock and subsequent weakening of the dimer interface. Others have shown that mutation of Tyr49 to alanine leads to unstable GST dimers.³⁴ Remarkably, the major disruptions caused to the GST structure could be reversed by back soaking GSH into crystals that were previously treated with PAO only.

The arsenic-based complexes presented here highlight the necessity to design and develop a novel drug that inhibits the enzyme at both the active site and the dimer interface to be as effective and optimal as possible. The GSTP1-1 PAO GSH structure described here provides a framework for the design of such compounds.

Materials and Methods

Materials

Wild-type GSTP1-1 and mutants were expressed in *E. coli* and purified as described previously.⁴⁷

Stability of PA(GS)₂ complex and kinetic studies with GSTP1-1

The instability constant $K_{\text{inst}} = \frac{[\text{GSH}]^2[\text{PAO}]}{[\text{PA}(\text{GS})_2]}$ was calculated by adding step-by-step GSH to a fixed concentration of PAO (60 μM) in potassium phosphate buffer 0.1M pH 6.5 and recording absorbance at 273 nm to quantify the amount of the formed complex. Inhibition experiments of PA(GS)₂ on GSTP1-1 were performed by incubating 1 μg of enzyme in 0.1M potassium phosphate buffer pH 6.5 (25°C) with variable amounts of GSH at fixed 1 mM CDNB at three different fixed PA(GS)₂ concentrations. Reaction rates were recorded at 340 nm.

Fluorescence study

The quenching of intrinsic fluorescence of enzyme (excitation wavelength 295 nm, emission wavelength 344 nm) was measured in a single photon counting

spectrofluorometer Fluoromax-4 Horiba, after the addition of variable amounts of PAO and enzyme.

Crystallization

GSTP1-1 was expressed, purified, and crystallized as described previously.⁴⁴ Cocrystallization experiments were not attempted because dithiothreitol (DTT), an essential ingredient for crystallization, would react with PAO. (GST P1-1 crystals only grow in reducing conditions, likely due to the two highly reactive surface cysteines in each monomer of the GST dimer). PAO (Sigma-Aldrich) was dissolved in dimethyl sulfoxide (DMSO) to make a 20 mM stock solution. Aliquots of the stock were added to a reservoir solution and diluted to a final concentration of 0.2–2.0 mM PAO. Crystals were transferred to 2 μL drops and left to soak for periods of several hours to a week.

Structure determination

Unless otherwise stated all data sets were processed with MOSFLM⁴⁸ and scaled with the program SCALA.⁴⁹ The structures were solved by molecular replacement using PHASER⁵⁰ with a model of GSTP1-1 complexed to GSH (PDB id: 5GSS) as a probe. Model building was done with COOT,⁵¹ interspersed by rounds of positional and isotropically restrained B-factor refinement using Phenix Refine.⁵² A summary of the data collection and refinement statistics and molprobit⁵³ analysis for all structures, including their quality relative to other structures at similar resolutions, is provided in Supporting Information Table S2.

XAS studies

Results from the mass spectrometry suggested that interaction of PAO with the protein at a single site per monomer was optimal at 2:1 ratio of PAO for 10 h. XAS data were recorded at 20 K on beamline 20B at the Photon Factory (Tsukuba, Japan). K-edge As XAS were measured in fluorescence detection mode using a 36-element Ge monolithic pixel array detector (Eurisy).

Mass spectrometry studies

Reaction mixtures were analyzed by electrospray mass spectrometry on an Agilent 6510 Q-TOF LC/MS (Bio21 Institute, Melbourne University).

Statistical Analysis

All experiments were performed in triplicate (i.e. on three distinct samples). Errors are given as SEM. Kinetics and spectroscopic data were analyzed by GraphPad Prism software (La Jolla, CA).

Accession Numbers

The models have been deposited in the Protein Data Bank (<http://www.rcsb.org/pdb/>) under the accession

numbers 5DCG (apo GSTP1-1), 5DAL (PAO-GSH complex), 5DAK (PAO complex, no GSH), and 5DDL (PAO complex soaked into crystals and back-soaked with GSH).

Acknowledgments

The authors thank Tilman Schmachtel and Volker Ullrich for suggesting to us that GSTP1-1 might bind PAO and encouraging us to pursue these studies; Mike Gorman and Guido Hansen for advice and encouragement and Nancy Hancock for protein production; BioCARS staff at the Advanced Photon Source and the staff at the Australian Synchrotron for their help. Use of the Advanced Photon Source was supported by the U.S. DOE, Basic Energy Sciences, Office of Energy Research. This research was partly undertaken on the MX1 and MX2 beamlines at the Australian Synchrotron, Victoria, Australia. The XAS was undertaken at the Australian National Beamline Facility at the Photon Factory in Japan, operated by the Australian Synchrotron.

References

1. Sheehan D, Meade G, Foley VM, Dowd CA (2001) Structure, function and evolution of glutathione transferases: implications for classification of non-mammalian members of an ancient enzyme superfamily. *Biochem J* 360:1-16.
2. Hayes JD, Flanagan JU, Jowsey IR (2005) Glutathione transferases. *Annu Rev Pharmacol Toxicol* 45:51-88.
3. Mannervik B, Castro VM, Danielson UH, Tahir MK, Hansson J, Ringborg U (1987) Expression of class Pi glutathione transferase in human malignant melanoma cells. *Carcinogenesis* 8:1929-1932.
4. Townsend DM, Tew KD (2003) The role of glutathione-S-transferase in anti-cancer drug resistance. *Oncogene* 22:7369-7375.
5. Gallagher RE (1998) Arsenic—new life for an old potion. *N Engl J Med* 339:1389-1391.
6. Larson RA, Kondo K, Vardiman JW, Butler AE, Golomb HM, Rowley JD (1984) Evidence for a 15;17 translocation in every patient with acute promyelocytic leukemia. *Am J Med* 76:827-841.
7. Kwong YL, Todd D (1997) Delicious poison: arsenic trioxide for the treatment of leukemia. *Blood* 89:3487-3488.
8. Bradley D (2000) Therapeutic needs revive arsenic compound. *Pharm Sci Technol Today* 3:401.
9. Murgo AJ (2001) Clinical trials of arsenic trioxide in hematologic and solid tumors: overview of the National Cancer Institute Cooperative Research and Development Studies. *Oncologist* 6: 22-28.
10. Bahlis NJ, McCafferty-Grad J, Jordan-McMurry I, Neil J, Reis I, Kharfan-Dabaja M, Eckman J, Goodman M, Fernandez HF, Boise LH, Lee KP (2002) Feasibility and correlates of arsenic trioxide combined with ascorbic acid-mediated depletion of intracellular glutathione for the treatment of relapsed/refractory multiple myeloma. *Clin Cancer Res* 8:3658-3668.
11. Akao Y, Yamada H, Nakagawa Y (2000) Arsenic-induced apoptosis in malignant cells in vitro. *Leuk Lymph* 37:53-63.
12. Zhang TC, Cao EH, Li JF, Ma W, Qin JF (1999) Induction of apoptosis and inhibition of human gastric cancer MGC-803 cell growth by arsenic trioxide. *Eur J Cancer* 35:1258-1263.
13. Woo SH, Park IC, Park MJ, Lee HC, Lee SJ, Chun YJ, Lee SH, Hong SI, Rhee CH (2002) Arsenic trioxide induces apoptosis through a reactive oxygen species-dependent pathway and loss of mitochondrial membrane potential in HeLa cells. *Int J Oncol* 21:57-63.
14. Lee TC, Wei ML, Chang WJ, Ho IC, Lo JF, Jan KY, Huang H (1989) Elevation of glutathione levels and glutathione S-transferase activity in arsenic-resistant Chinese hamster ovary cells. *In Vitro Cell Dev Biol* 25: 442-448.
15. Wang Z, Dey S, Rosen BP, Rossman TG (1996) Efflux-mediated resistance to arsenicals in arsenic-resistant and -hypersensitive Chinese hamster cells. *Toxicol Appl Pharmacol* 137:112-119.
16. Romach EH, Zhao CQ, Del Razo LM, Cebrian ME, Waalkes MP (2000) Studies on the mechanisms of arsenic-induced self tolerance developed in liver epithelial cells through continuous low-level arsenite exposure. *Toxicol Sci* 54:500-508.
17. Lo JF, Wang HF, Tam MF, Lee TC (1992) Glutathione S-transferase pi in an arsenic-resistant Chinese hamster ovary cell line. *Biochem J* 288: 977-982.
18. Wang HF, Lee TC (1993) Glutathione S-transferase pi facilitates the excretion of arsenic from arsenic-resistant Chinese hamster ovary cells. *Biochem Biophys Res Commun* 192:1093-1099.
19. Liu J, Chen H, Miller DS, Saavedra JE, Keefer LK, Johnson DR, Klaassen CD, Waalkes MP (2001) Overexpression of glutathione S-transferase II and multidrug resistance transport proteins is associated with acquired tolerance to inorganic arsenic. *Mol Pharmacol* 60:302-309.
20. Jing Y, Dai J, Chalmers-Redman RM, Tatton WG, Waxman S (1999) Arsenic trioxide selectively induces acute promyelocytic leukemia cell apoptosis via a hydrogen peroxide-dependent pathway. *Blood* 94:2102-2111.
21. Lu M, Xia L, Luo D, Waxman S, Jing Y (2004) Dual effects of glutathione-S-transferase pi on As₂O₃ action in prostate cancer cells: enhancement of growth inhibition and inhibition of apoptosis. *Oncogene* 23:3945-3952.
22. Zhou L, Jing Y, Styblo M, Chen Z, Waxman S (2005) Glutathione-S-transferase pi inhibits As₂O₃-induced apoptosis in lymphoma cells: involvement of hydrogen peroxide catabolism. *Blood* 105:1198-1203.
23. Kitchin KT (2001) Recent advances in arsenic carcinogenesis: modes of action, animal model systems, and methylated arsenic metabolites. *Toxicol Appl Pharmacol* 172:249-261.
24. Xie Y, Liu J, Liu Y, Klaassen CD, Waalkes MP (2004) Toxicokinetic and genomic analysis of chronic arsenic exposure in multidrug-resistance *mdr1a/1b*(-/-) double knockout mice. *Mol Cell Biochem* 255:11-18.
25. Leslie EM, Haimeur A, Waalkes MP (2004) Arsenic transport by the human multidrug resistance protein 1 (MRP1/ABCC1). Evidence that a tri-glutathione conjugate is required. *J Biol Chem* 279:32700-32708.
26. Oetken C, von Willebrand M, Marie-Cardine A, Pessa-Morikawa T, Stahls A, Fisher S, Mustelin T (1994) Induction of hyperphosphorylation and activation of the p56lck protein tyrosine kinase by phenylarsine oxide, a phosphotyrosine phosphatase inhibitor. *Mol Immunol* 31:1295-1302.
27. Estrov Z, Manna SK, Harris D, Van Q, Estey EH, Kantarjian HM, Talpaz M, Aggarwal BB (1999) Phenylarsine oxide blocks interleukin-1beta-induced

- activation of the nuclear transcription factor NF-kappaB, inhibits proliferation, and induces apoptosis of acute myelogenous leukemia cells. *Blood* 94:2844–2853.
28. Larochette N, Decaudin D, Jacotot E, Brenner C, Marzo I, Susin SA, Zamzami N, Xie Z, Reed J, Kroemer G (1999) Arsenite induces apoptosis via a direct effect on the mitochondrial permeability transition pore. *Exp Cell Res* 249:413–421.
 29. Sahara N, Takeshita A, Kobayashi M, Shigeno K, Nakamura S, Shinjo K, Naito K, Maekawa M, Horii T, Ohnishi K others (2004) Phenylarsine oxide (PAO) more intensely induces apoptosis in acute promyelocytic leukemia and As2O3-resistant APL cell lines than As2O3 by activating the mitochondrial pathway. *Leuk Lymph* 45:987–995.
 30. Horsley L, Cummings J, Middleton M, Ward T, Backen A, Clamp A, Dawson M, Farmer H, Fisher N, Halbert G, Halford S, Harris A, Hasan J, Hogg P, Kumaran G, Little R, Parker GJ, Potter P, Saunders M, Roberts C, Shaw D, Smith N, Smythe J, Taylor A, Turner H, Watson Y, Dive C, Jayson GC, Cancer Research UK Drug Development Office Phase I clinical trial (2013) A phase 1 trial of intravenous 4-(*N*-(*S*-glutathionylacetyl)amino) phenylarsenoxide (GSAO) in patients with advanced solid tumours. *Cancer Chemother Pharmacol* 72:1343–1352.
 31. Ricci G, Lo Bello M, Caccurri AM, Pastore A, Nuccetelli M, Parker MW, Federici G (1995) Site-directed mutagenesis of human glutathione transferase P1-1. Mutation of Cys-47 induces a positive cooperativity in glutathione transferase P1-1. *J Biol Chem* 270:1243–1248.
 32. Wilce MC, Parker MW (1994) Structure and function of glutathione *S*-transferases. *Biochim Biophys Acta* 1205:1–18.
 33. Oakley AJ, Lo Bello M, Battistoni A, Ricci G, Rossjohn J, Villar HO, Parker MW (1997) The structures of human glutathione transferase P1-1 in complex with glutathione and various inhibitors at high resolution. *J Mol Biol* 274:84–100.
 34. Hegazy UM, Mannervik B, Stenberg G (2004) Functional role of the lock and key motif at the subunit interface of glutathione transferase p1-1. *J Biol Chem* 279:9586–9596.
 35. Ricci G, Caccurri AM, Lo Bello M, Rosato N, Mei G, Nicotra M, Chiessi E, Mazzetti AP, Federici G (1996) Structural flexibility modulates the activity of human glutathione transferase P1-1. Role of helix 2 flexibility in the catalytic mechanism. *J Biol Chem* 271:16187–16192.
 36. Hitchens TK, Mannervik B, Rule GS (2001) Disorder-to-order transition of the active site of human class Pi glutathione transferase, GST P1-1. *Biochemistry* 40:11660–11669.
 37. Stella L, Caccurri AM, Rosato N, Nicotra M, Lo Bello M, De Matteis F, Mazzetti AP, Federici G, Ricci G (1998) Flexibility of helix 2 in the human glutathione transferase P1-1. time-resolved fluorescence spectroscopy. *J Biol Chem* 273:23267–23273.
 38. Munro KL, Mariana A, Klavins AI, Foster AJ, Lai B, Vogt S, Cai Z, Harris HH, Dillon CT (2008) Microprobe XRF mapping and XAS investigations of the intracellular metabolism of arsenic for understanding arsenic-induced toxicity. *Chem Res Toxicol* 21:1760–1769.
 39. Talemi SR, Jacobson T, Garla V, Navarrete C, Wagner A, Tamas MJ, Schaber J (2014) Mathematical modeling of arsenic transport, distribution and detoxification processes in yeast. *Mol Microbiol* 92:1343–1356.
 40. Allen FH (2002) The Cambridge Structural Database: a quarter of a million crystal structures and rising. *Acta Cryst B* 58:380–388.
 41. Ang WH, Parker LJ, De Luca A, Juillerat-Jeanneret L, Morton CJ, Lo Bello M, Parker MW, Dyson PJ (2009) Rational design of an organometallic glutathione transferase inhibitor. *Angew Chem Int Ed Engl* 48:3854–3857.
 42. Cesareo E, Parker LJ, Pedersen JZ, Nuccetelli M, Mazzetti AP, Pastore A, Federici G, Caccurri AM, Ricci G, Adams JJ, Parker MW, Lo Bello M (2005) Nitrosylation of human glutathione transferase P1-1 with dinitrosyl diglutathionyl iron complex in vitro and in vivo. *J Biol Chem* 280:42172–42180.
 43. Oakley AJ, Lo Bello M, Nuccetelli M, Mazzetti AP, Parker MW (1999) The ligandin (non-substrate) binding site of human Pi class glutathione transferase is located in the electrophile binding site (H-site). *J Mol Biol* 291:913–926.
 44. Parker LJ, Ciccone S, Italiano LC, Primavera A, Oakley AJ, Morton CJ, Hancock NC, Bello ML, Parker MW (2008) The anti-cancer drug chlorambucil as a substrate for the human polymorphic enzyme glutathione transferase P1-1: kinetic properties and crystallographic characterisation of allelic variants. *J Mol Biol* 380:131–144.
 45. Parker LJ, Italiano LC, Morton CJ, Hancock NC, Ascher DB, Aitken JB, Harris HH, Campomanes P, Rothlisberger U, De Luca A, Lo Bello M, Ang WH, Dyson PJ, Parker MW (2011) Studies of glutathione transferase P1-1 bound to a platinum(IV)-based anticancer compound reveal the molecular basis of its activation. *Chemistry* 17:7806–7816.
 46. Ricci G, De Maria F, Antonini G, Turella P, Bullo A, Stella L, Filomeni G, Federici G, Caccurri AM (2005) 7-Nitro-2,1,3-benzoxadiazole derivatives, a new class of suicide inhibitors for glutathione *S*-transferases. Mechanism of action of potential anticancer drugs. *J Biol Chem* 280:26397–26405.
 47. Lo Bello M, Battistoni A, Mazzetti AP, Board PG, Muramatsu M, Federici G, Ricci G (1995) Site-directed mutagenesis of human glutathione transferase P1-1. Spectral, kinetic, and structural properties of Cys-47 and Lys-54 mutants. *J Biol Chem* 270:1249–1253.
 48. Leslie AW, Powell H. Processing diffraction data with mosflm. In: Read R, Sussman J, Ed. (2007) *Evolving Methods for Macromolecular Crystallography*, Vol. 245, Springer Netherlands: NATO Science Series. pp 41–51.
 49. Collaborative Computational Project N (1994) The CCP4 Suite: Programs for Protein Crystallography. *Acta Cryst D* 50:760–763.
 50. McCoy AJ, Grosse-Kunstleve RW, Adams PD, Winn MD, Storoni LC, Read RJ (2007) Phaser crystallographic software. *J Appl Cryst* 40:658–674.
 51. Emsley P, Cowtan K (2004) Coot: model-building tools for molecular graphics. *Acta Cryst D* 60:2126–2132.
 52. Adams PD, Afonine PV, Bunkoczi G, Chen VB, Davis IW, Echols N, Headd JJ, Hung LW, Kapral GJ, Grosse-Kunstleve RW, McCoy AJ, Moriarty NW, Oeffner R, Read RJ, Richardson DC, Richardson JS, Terwilliger TC, Zwart PH (2010) PHENIX: a comprehensive Python-based system for macromolecular structure solution. *Acta Cryst D* 66:213–221.
 53. Chen VB, Arendall WB, 3rd Headd JJ, Keedy DA, Immormino RM, Kapral GJ, Murray LW, Richardson JS, Richardson DC (2010) MolProbity: all-atom structure validation for macromolecular crystallography. *Acta Cryst D* 66:12–21.